Structure of the JET edge radial electric field in He and D plasmas

C. Silva[1], E. R. Solano[2], J. C. Hillesheim[3], E. Delabie[4], S. Aleiferis[5], G. Birkenmeier[6,7], L. Gil[1], C. Giroud[3], E. Litherland-Smith[3], R. B. Morales[3], D. Nina[1], A. Silva[1] and JET Contributors[*]

EUROfusion Consortium, JET, Culham Science Centre, Abingdon, OX14 3DB, UK
[1]Instituto de Plasmas e Fusão Nuclear, Instituto Superior Técnico, Universidade de Lisboa, Portugal
[2]Laboratorio Nacional de Fusión, CIEMAT, 28040 Madrid, Spain
[3]CCFE, Culham Science Centre, Abingdon, OX14 3DB, UK
[4]Oak Ridge National Laboratory, Oak Ridge, Tennessee 37831-6169, USA
[5]Institute for Nuclear and Radiological Science and Technology, Safety and Energy, NCSR Demokritos, 15310 Agia Paraskevi, Greece
[6]Max-Planck-Institut fur Plasmaphysik, Boltzmannstr. 2, D-85748 Garching, Germany
[7]Physics Department E28, Technical University Munich, James-Franck-Str. 1, 85748 Garching, Germany

Abstract

Perpendicular velocity, $v_\perp$, measurements have been obtained in JET experiments designed to investigate the underlying mechanisms influencing the L–H power threshold. L–H transitions were induced by using both NBI and ICRH in deuterium and helium plasmas. The $v_\perp$ profile in the low density branch of the L-H transition has a modest or even no well and a marked peak near the separatrix in NBI heated discharges for both D and He plasmas, with a sharper SOL peak for He plasmas. As the line-averaged density increases, the SOL $v_\perp$ peak decreases, in agreement with the modifications in the electron temperature profile at the divertor target, while the $v_\perp$ well becomes deeper. Nevertheless, even in the high density branch, a shallow $v_\perp$ well is found at the L-H transition, $v_\perp \sim 1$ - 2 km/s, which is lower by a factor of about two than the contribution from the diamagnetic term. No evidence for the existence of a critical value in $v_\perp$ is found at JET, particularly for helium plasmas. This may be explained by the existence of an edge toroidal flow relevant mainly at low density where the power threshold is high. In addition, no significant change in the edge $v_\perp$ is measured preceding the L-H transition.

[*]See the author list of 'Overview of JET results for optimising ITER operation' by J. Mailloux et al. to be published in Nuclear Fusion Special issue: Overview and Summary Papers from the 28th Fusion Energy Conference (Nice, France, 10-15 May 2021)"

1. Introduction

Regimes with improved energy and particle confinement, such as the H-mode, are being considered for a future fusion reactor. A minimum heating power is required to trigger a transition to the H-mode regime that exhibits a non-monotonic dependence on the density. Empirical scaling laws have been derived expressing the threshold power for the L–H transition, P_{LH}, in terms of plasma parameters such as magnetic field and electron density [1]. However, a considerable scatter exists in the experimental data as a consequence of the hidden parameters not included in the scaling law that can vary the power threshold by up to a factor of 2, having therefore a large impact on the prediction for future devices. It is also well known that the threshold power depends on the main ion species. ITER scenarios foresee an H-mode regime either in hydrogen, helium or suitable mixtures for its initial non-active phase of operation in order to study H-modes as early as possible [2]. The power threshold generally exhibits an inverse ion mass dependence that does not apply to helium. There are large uncertainties on the isotope mass effect on the L-H transition and even contradictory results, particularly for helium plasmas [3 - 7], calling for additional experiments.

The existence of a strong shear in the plasma flow perpendicular to the magnetic field caused by a radial electric field, E_r, is thought to be fundamental for the edge turbulence suppression, explaining the formation of the edge transport barrier and leading to the L-H transition. Detailed experimental evidence of the correlation between the E×B flow shear and the establishment of an edge transport barrier has been obtained in different devices (e.g. [8, 9]). Biasing experiments were particularly relevant as the radial electric field is applied externally to the edge plasma in a controlled way, permitting to establish a causality between shear flow and turbulence suppression (e.g. [10, 11]). The origin of the E_r×B flow is still not fully understood and therefore E_r measurements are essential to better understand the link between flow shear and turbulence suppression. Observations from different devices also suggest that the H-mode power threshold is influenced by the scrape-off layer (SOL) physics, for instance due to changes in the boundary conditions resulting from different divertor configurations (e.g. [12, 13]), indicating that the outer shear layer may be particularly relevant for the L-H transition. A large positive E_r spike near the separatrix depending on ion mass was seen in modelling results [14]. EDGE2D-EIRENE modeling of JET plasmas by changing hydrogen isotopes (H–D–T) showed that the

magnitude of the near SOL E_r is lower in H cases in which the H-mode threshold power is higher [14].

Several experimental observations have been reported recently on the E_r evolution near the L-H transition [7, 12, 13, 15 - 17]. Particularly relevant were the experiments performed on ASDEX Upgrade (AUG) where the relation between the macroscopic input power required to access the H-mode and the local E×B shear was investigated at various toroidal magnetic fields, different electron densities, and in both hydrogen and deuterium plasmas [16, 18]. For the H-mode onset, a threshold in the E×B flow minimum of 6.7±1.0 km/s was found, identifying the $v_{E\times B}$ velocity and not E_r as the critical player for the L-H transition. These results are in contrast with JET observations of a shallow E_r well at the L–H transition [12]. At JET, the E×B flow minimum was found to be in the order of 0.5–1 km/s despite variations in edge density, toroidal magnetic field, divertor configuration or wall composition. However, JET results were limited by the accuracy of the poloidal impurity ion flow measurements.

This contribution focuses on the characterization of the edge $v_\perp$ when approaching the L-H transition on JET with different ion species, contributing to a better understanding of the transition physics and its triggering mechanisms. To this purpose, detailed measurements were obtained by Doppler backscattering in experiments designed to determine the effect of the main ion species mass in the L–H power threshold physics and scaling [19]. The correlation between the $v_\perp$ profile just before the confinement transition and the power threshold is investigated in deuterium and helium plasmas. A shallow $v_\perp$ well is measured at the L-H transition, $v_\perp \sim 1.5$ km/s, which is lower by a factor of two than the contribution from the diamagnetic term. Furthermore, no evidence for the existence of a critical $v_\perp$ is found at JET. This may be explained by the existence of an edge toroidal flow relevant mainly at low density where the power threshold is high.

2. Description of the experiment

Doppler backscattering (DBS) is a microwave diagnostic for density fluctuation measurements that measures the radially localized propagation velocity and fluctuation level of intermediate wavenumber turbulent structures. Motion of the density turbulence near the cutoff layer induces a Doppler frequency shift (f_D) in the backscattered signal given by $f_D = v_\perp k_\perp/2\pi$, where $v_\perp = v_{E\times B} + v_{phase}$ is the perpendicular velocity of the turbulence moving in the plasma, $k_\perp$ is the perpendicular wavenumber and v_{phase} the phase

velocity of the fluctuations. For the edge plasma, the E×B velocity term generally dominates (e.g. [20, 21]) and the radial electric field can be obtained. The scattering wavenumber of the density fluctuations is determined via ray tracing [22]. For the data presented here the probed $k_\perp$ is ~ 5.5 cm^{-1} around the pedestal region for discharges in horizontal target configuration (plasmas with the outer divertor strike-point in the horizontal target).

The JET correlation reflectometer [23, 24] consists of two X-mode fast frequency hopping (≤ 60 μs) channels launched from the LFS midplane with probing frequencies variable in the range 75 – 110 GHz (W-band) and another two channels operating either in the F- (90 – 140 GHz) or V-band (50 – 75 GHz). Particularly relevant for this work are probing frequencies in the V-band, permitting the extension of the diagnostic measurement capability across the separatrix up to the SOL and thus the determination of both inner and outer shear layer. Each channel can be pre-programmed with a specified launch frequency pattern, which is repeated continuously throughout the discharge, allowing a radial scan of the measurement location.

For the data presented here, the reflectometer channel 1 (master) was typically set to a 14 point frequency sweep, while channel 2 (slave) had an 11 point frequency sweep of 2 ms duration around each master frequency with the full frequency sweep taking 308 ms. DBS measurements presented in this paper are taken in the last full sweep of the probing frequency before the first L-H transition. Dithers and divertor oscillations are sometimes observed near the L-H transition (e.g. [13]) leading to modulations in the edge perpendicular flow profile. As stationary periods are required to obtain a reliable $v_\perp$ profile, measurements are performed before such events in case they are present. The analysis presented here was performed with the DBS slave signals to obtain a higher spatial resolution. The Doppler frequency is obtained from the complex amplitude spectrum of the reflectometer signals by a sliding FFT method using different methods (spectrum weighted mean, Gaussian fit or a fit to the asymmetric part of the power spectrum, e.g. [20]). For the measurements presented here the typical uncertainty in $v_\perp$ is in order of 0.5 km/s. An electron density radial profile averaged over the DBS sweep time obtained with the profile reflectometry system is used to localize the measurements and as ray tracing input to determine $k_\perp$. The radial error bar resulting from the location of the probing frequency for each frequency step is generally less than 5 mm (estimated as the standard deviation of the probing frequency location over the DBS sweep time).

Over the years, several L–H threshold experiments were performed on JET to investigate the importance of different parameters such as plasma current, divertor geometry and isotopic mass [12, 13, 19, 25, 26]. Here we report on measurements obtained in line-averaged density scans at 2.4 T / 2 MA in deuterium and helium plasmas with the outer divertor strike-point in the horizontal target [19]. The L–H transitions were induced by slowly increasing the heating power using either NBI or ICRH. As reported in [19], the He power threshold in the low density branch is about $2\times P_{LH}$ in D, while in the high density branch the P_{LH} of D and He are approximately aligned.

3. Density scan in helium NBI heated plasmas

In this section we start by analysing the dependence of the perpendicular velocity measured by DBS at the L-H transition on the line-averaged electron density for helium plasmas. A series of six NBI heated discharges were selected with different values of line-averaged electron density, ranging from the low to the high density branch of the L-H transition, with a minimum P_{LH} at a density of $\bar{n} \approx 4.5 - 5\times10^{19}$ m^{-3}. Figure 1 presents the $v_\perp$ radial profile for different values of line-averaged electron density together with the electron density radial profile obtained with the profile reflectometry system. The $v_\perp$ profile in the low density branch exhibits a modest or even no well but shows a marked outer peak with $v_\perp$ up to 3.5 km/s and a width of ≈1 cm. This marked positive peak at the separatrix and in the near SOL is most probably associated with a fast radial decay of the target electron temperature (effect of the Debye sheath drop at the target of $\sim 3T_e/e$). The SOL peak decreases with increasing line-averaged electron density, which is consistent with the expected variation of the divertor conditions as will be shown in section 8.

In contrast, the $v_\perp$ well becomes stronger with line-averaged electron density and, consequently, the $v_\perp$ minimum varies along the density scan. Nevertheless, even for the highest density, the perpendicular velocity shows a shallow well at the L-H transition, in the order of 1.2 km/s. This contrasts with AUG observations where a critical minimum $v_\perp$ was reported for D and H plasmas with a much higher value, $v_\perp \approx 6.7$ km/s, independent of density.

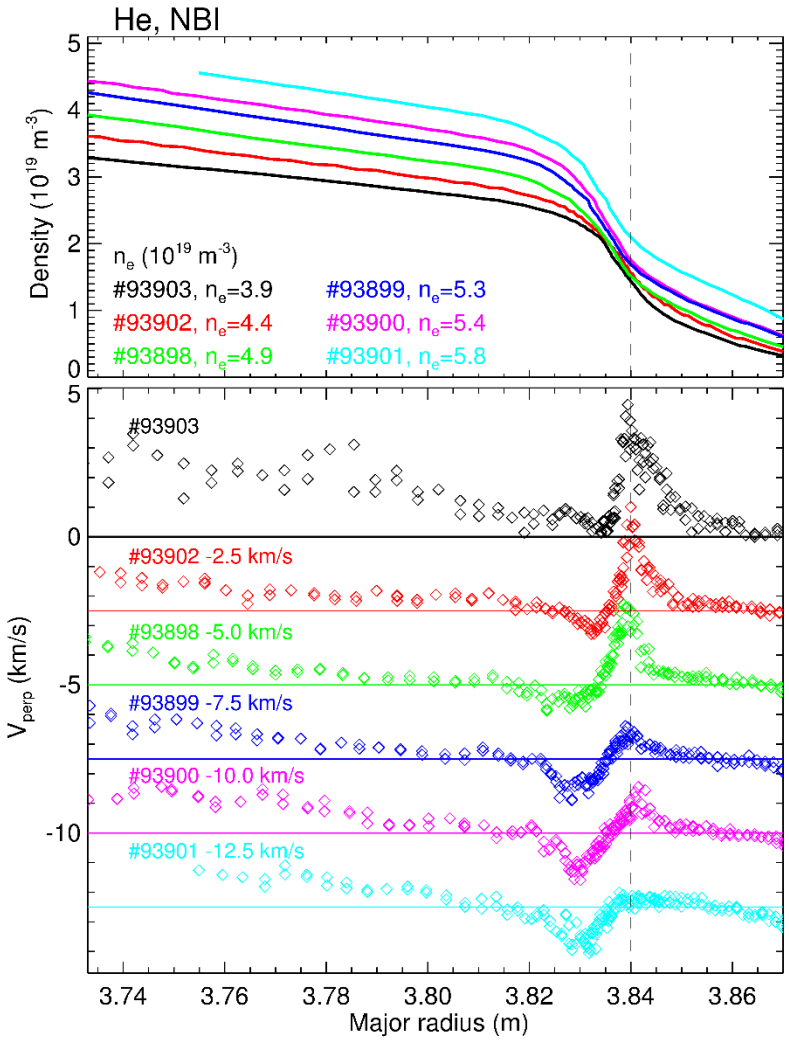

Figure 1: Radial profiles of electron density and mean perpendicular velocity for different values of line-averaged electron density for helium NBI heated plasmas. For clarity, each $v_\perp$ profile is offset by 2.5 km/s. The separatrix (dashed line) is at 3.84 (±0.01) m. The NBI power at the L–H transition in order of increasing line-averaged density are as follows: 93903 (P_{NBI} ~7.4 MW), 93902 (P_{NBI} ~4.4 MW), 93898 (P_{NBI} ~3.0 MW), 93899 (P_{NBI} ~4.8 MW), 93900 (P_{NBI} ~5.9 MW), 93901 (P_{NBI} ~7.4 MW).

4. Density scan in deuterium with ICRH and NBI heating

Our attention is now turned to a line-averaged density scan in deuterium plasmas with NBI heating. In this case the minimum P_{LH} is around $\bar{n} \approx 3\times10^{19}$ m^{-3}. Figure 2 presents the radial profile of the electron density and mean perpendicular velocity for different values of line-averaged density. As illustrated, the behavior in D is generally similar to that reported above for He plasmas, although with a smaller and broader outer $v_\perp$ peak. The SOL peak disappears at high densities, likely as a consequence of the reduction in the

temperature radial gradient at the divertor target as will be shown in section 8. For the lowest density value, the $v_\perp$ well has a positive minimum similarly to what is observed in He plasmas. The remaining profiles in the density scan are similar, showing again a shallow well at the L-H transition, in the order of 1.3 km/s.

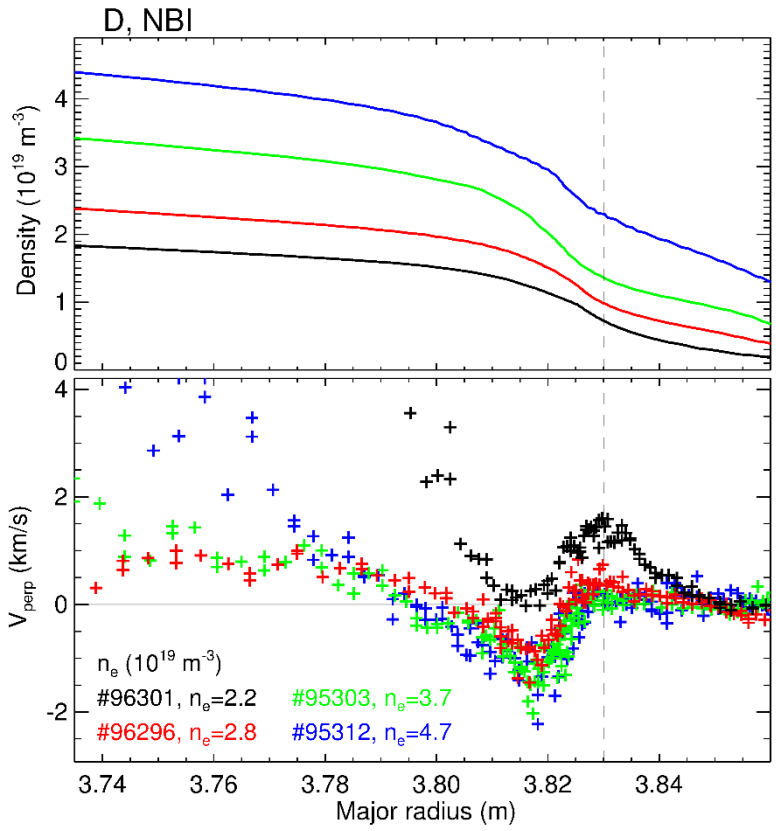

Figure 2: Radial profiles of electron density and mean perpendicular velocity for different values of line-averaged electron density for deuterium NBI heated deuterium plasmas. The separatrix (dashed line) is at 3.83 (±0.01) m. The NBI power at the L–H transition in order of increasing line-averaged density are as follows: 96301 (P_{NBI} ~3.3 MW), 96296 (P_{NBI} ~2.5 MW), 95303 (P_{NBI} ~4.0 MW), 95312 (P_{NBI} ~5.0 MW).

As illustrated in figures 1 and 2, at low line-average density, the $v_\perp$ profile is generally shifted upward possibly due to the torque induced by NBI. This shift decreases with line-averaged density suggesting the existence of a similar trend in the rotation induced by NBI. This is consistent with AUG data where the toroidal velocity at the edge in L-mode was reported to decrease strongly with increasing density [27].

L-H transition experiments were also performed in ICRH only heated discharges, which are particularly relevant due to the absence of external torque. Figure 3 presents the radial profile of the electron density and mean perpendicular velocity at the L-H transition for

different values of line-averaged density in ICRH heated deuterium plasmas. Again the outer peak in the flow reduces with density, as expected from the reduction of the divertor target electron temperature. Compared to the NBI heated case, the depth of the flow well has a much weaker dependence on the line-averaged density possibly due the absence of an external torque. However, a small upward shift is still seen for the lowest density discharge. Again, no critical minimum $v_\perp$ is found at the transition even in ICRH only heated discharges, although in this case the variation with density is modest. Interestingly, the shape of the $v_\perp$ profile in the well region is very similar across the density scan. When vertically shifted to match the minimum $v_\perp$, profiles are found to be similar almost up to the separatrix (see figure 3c), suggesting that the offset, possibly caused by the toroidal rotation, may not be important for the L-H transition.

As illustrated in figure 3c, the flow velocity around the separatrix decreases with line-averaged density. This suggests that the outer shear does not play a major role in the transition in spite of the changes in the boundary conditions and in the outer flow shear. In the high density branch, the outer shear is reduced and the power threshold rises as the line-averaged density is increased. However, this is not the case in the low density branch and therefore no clear correlation is found between the outer flow shear and the power threshold. In addition, the minimum in the power threshold occurs for pulse #96288 where no SOL peak is observed.

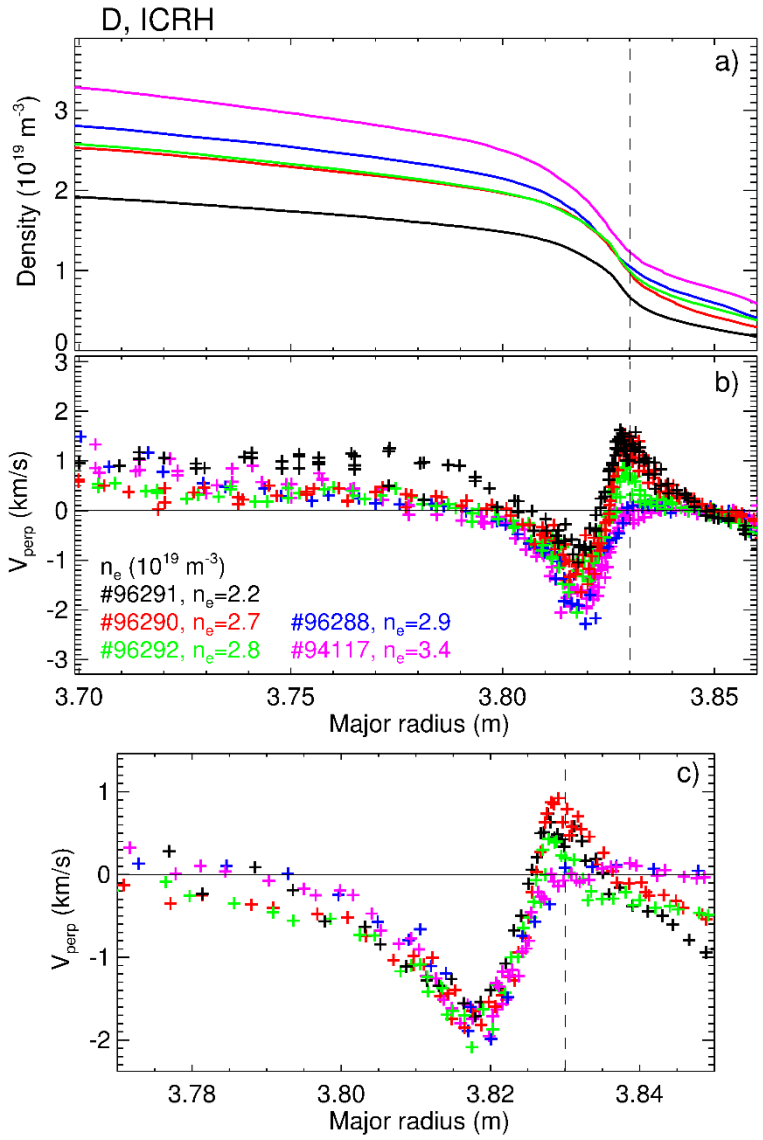

Figure 3: Radial profiles of electron density (a) and mean perpendicular velocity (b and c) for different values of line-averaged electron density for deuterium ICRH heated deuterium plasmas. Profiles in c) were vertically shifted to match the minimum $v_\perp$. The separatrix (dashed line) is at 3.83 (±0.01) m. The ICRH power at the L–H transition in order of increasing line-averaged density are as follows: 96291 (P_{ICRH} ~3.4 MW), 96290 (P_{ICRH} ~2.5 MW), 96292 (P_{ICRH} ~2.8 MW), 96288 (P_{ICRH} ~2.7 MW), 94117 (P_{ICRH} ~3.1 MW).

The edge perpendicular flow profile is now compared for NBI and ICRH heated deuterium plasmas (see figure 4). As illustrated, the edge $v_\perp$ profile has small differences in NBI and ICRH heated plasmas except at low density in the region inside the separatrix where they differ significantly, possibly due to the plasma rotation induced by NBI. This confirms that the effect of NBI torque is seen mainly at low line-averaged density and may not be relevant for the transition (at least for deuterium plasmas where the P_{LH} is low). This hypothesis is consistent with the observation that no significant difference in P_{LH} is found

between NBI heated (with additional torque) and ICRH heated (no additional torque) deuterium plasmas, as previously reported at JET [12, 25]. It was concluded that the flow shear driven by the toroidal rotation profile does not appear to play a role in setting the edge transport barrier [12].

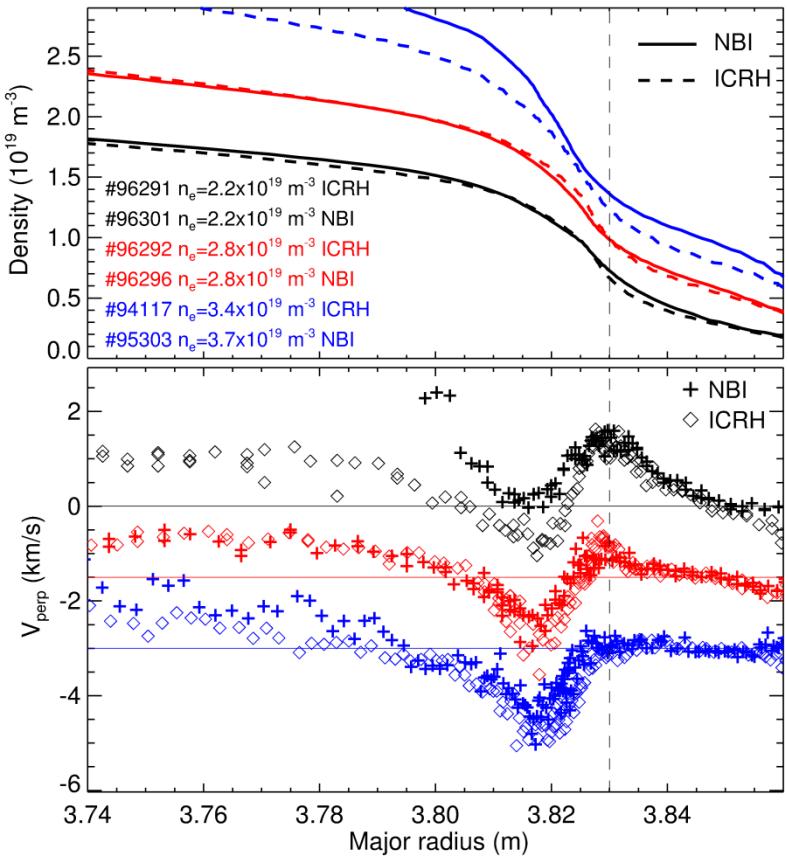

Figure 4: Radial profiles of electron density and mean perpendicular velocity for different values of line-averaged electron density for deuterium plasmas with NBI and ICRH deuterium heating. For clarity, the $v_\perp$ profile at different densities are offset by 1.5 km/s. The separatrix (dashed line) is at 3.83 (±0.01) m.

5. Determination of the velocity shear

In this section our experimental results are further discussed to clarify the importance of the E×B flow shear, which is the most relevant quantity to understand the L-H transition. Measurements are available from the pedestal region across the separatrix up to the SOL, thus permitting the determination of both inner and outer shear layer, which may both be relevant for the L-H transition. The flow shear was estimated from the $v_\perp$ profile obtained near the L-H transition in the inner and outer shear regions, respectively inside (outside) the $v_\perp$ well in the negative (positive) shear region. The flow velocity was determined at

three radial locations (separatrix, well and density pedestal) and then the shear estimated using the following proxies: outer shear = ($v_\perp^{sep}$ - $v_\perp^{well}$)/ΔR; inner shear = ($v_\perp^{ped}$ - $v_\perp^{well}$)/ΔR. The average shear (average of the inner and outer shear) was also estimated to assess the possible importance of an effective shear in the entire steep edge density gradient region from the separatrix up to the pedestal top.

The dependence of the shear on the line-averaged electron density is presented in figure 5. Although both $v_\perp^{sep}$ and $v_\perp^{well}$ generally decrease with line-averaged electron density, the variation is larger for $v_\perp^{sep}$ leading to a reduction of the outer shear with density (except for D NBI heated plasmas). This indicates that the $v_\perp$ separatrix peak, largely defined by the divertor conditions, impacts strongly on the outer shear. Our results suggest that the outer shear does not play a major role in defining P_{LH} as it varies with density. The inner shear exhibits a significant variation with line-averaged density for helium plasmas but not for deuterium plasmas. A critical value of the inner shear might therefore exist for deuterium plasmas taking into account the uncertainties of the measurements. As illustrated in figure 5c, the average shear has a modest variation (within the error bars) across each of the density scans. Therefore, these observations would be consistent with the existence of a critical effective shear across the edge plasma. The lower average shear for deuterium NBI heated plasmas results mainly from its shallower $v_\perp$ well when compared to ICRH heated plasmas.

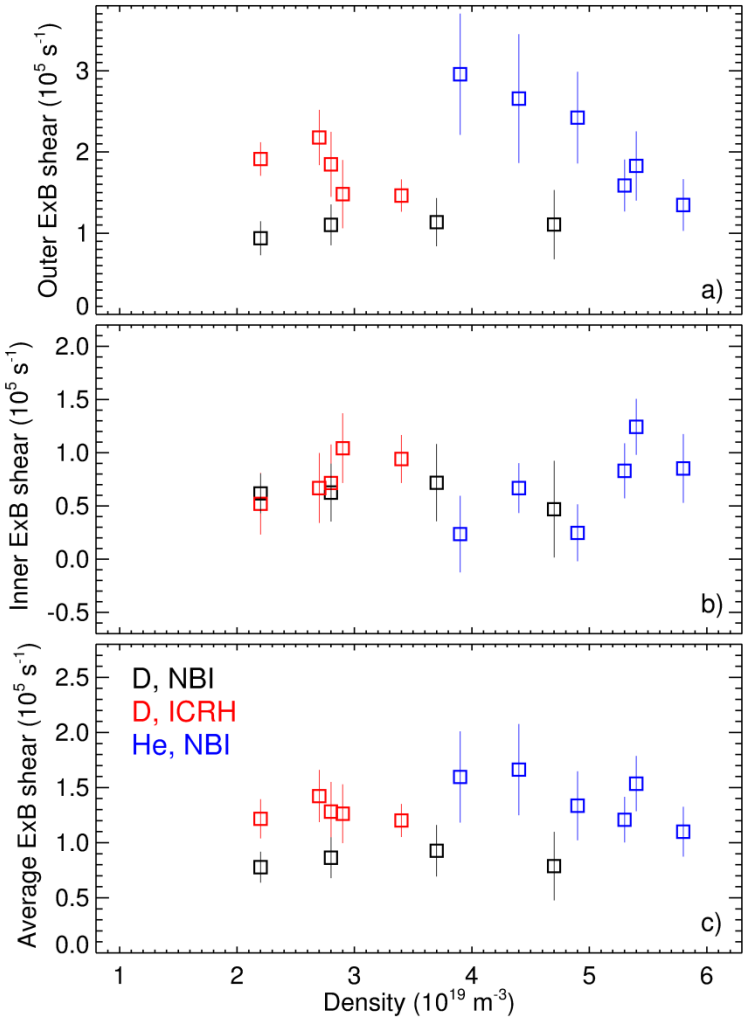

Figure 5: Outer, inner and average E×B flow shear at the L-H transition estimated from DBS $v_\perp$ measurements at the separatrix, well and pedestal regions.

6. Contribution of the diamagnetic term

To better understand the role of the edge E_r in the L–H power threshold, the diamagnetic contribution, $E_{r,dia} = \nabla p_i/(Z_i e n_i)$, is estimated. Since edge CXRS data is rarely available for the dataset used here and absent for the ICRH only heated discharges, $E_{r,dia}$ is estimated from the electron kinetic profiles using $E_{r,dia} = \nabla p_e/(2en_e)$ for helium and $E_{r,dia} = \nabla p_e/(en_e)$ for deuterium assuming $T_i = T_e$, which is the case for JET plasmas near the pedestal top region [12] but it is unclear if this is also the case at the separatrix. The T_e profiles are obtained from HRTS and ECE data, while reflectometry was used for electron density profiles.

The minimum value of $E_{r,dia}$ at the L-H transition is displayed in figure 6a for the density scan in deuterium ICRH heated plasmas. For reference P_{LH} and the E_r minimum measured

by DBS are also shown. Following the conventions for the evaluation of the L-H power threshold, the loss power is expressed as $P_{loss} = P_{in}$ - dW/dt, where the dW/dt represents the change in the plasma energy content. Further information on the power threshold evaluation for the experiments reported here can be found in [19]. As illustrated in figure 6a, although the minimum of $E_{r,dia}$ appears to follow that of P_{loss}, its variation over the explored density range is small and within the error bars. Therefore, our observations would be consistent with the assumption of a critical $E_{r,dia}$.

The E_r measured by DBS is clearly lower than the contribution from the diamagnetic term estimated from electron temperature by a factor of about two in the high density branch and by an even larger factor in the low density branch. This may indicate that the edge poloidal and/or toroidal velocities also have a relevant contribution to the perpendicular flow. Another possibility is that the diamagnetic term is overestimated by assuming $T_i = T_e$. The value of the separatrix T_i influences the determination of the diamagnetic term as temperature gradients are modest in L-mode. $T_i > T_e$ at the separatrix has been observed in a number of tokamaks with T_i/T_e varying with the macroscopic parameters such as the plasma density or heating power [28]. Different studies show a drop of T_i/T_e with increasing density, consistent with the increase of the ion–electron thermal coupling [28]. Unfortunately, T_i measurements are not available at JET in the region relevant for this study (just inside the separatrix). Assuming for instance $T_i = T_e$ in the pedestal top region and $T_i = 1.5T_e$ at the separatrix would reduce the T_i gradient by a factor of about two with respect to the case with $T_{i,sep} = T_{e,sep}$. Consequently, this effect might be relevant, particularly at low density where the ion–electron heat exchange coupling is weaker.

The dependence of the diamagnetic term on the line-averaged density for NBI heated helium plasmas is presented in figure 6b together with P_{LH} and the E_r minimum measured by DBS. Although the $E_{r,dia}$ minimum does not vary significantly within the high density branch, it is clearly larger at low density mainly due to the higher P_{LH} characteristic of the low density branch. This leads to a larger edge T_e radial gradient and translates into a deeper $E_{r,dia}$ well. Once more, the observed $v_\perp$ is clearly lower than the contribution from the diamagnetic term (by a factor of about two in the high density branch).

As illustrated in figure 6b, the $E_{r,dia}$ dependence on the line-averaged density is not well correlated with the DBS-measured E_r minimum. However, this may be explained by the existence of an edge toroidal flow mainly relevant at low density. The edge toroidal flow is expected to be proportional to P_{LH} in NBI heated discharges and to decrease with line-averaged density justifying the large discrepancy between observed edge perpendicular

flow and the diamagnetic contribution in the low density branch. Although no edge CXRS measurements exist, data from the core system is available up to ρ=0.85. Indeed, the toroidal rotation at ρ=0.85 is larger by a factor of 2 to 3 in the low density branch than in the high density branch.

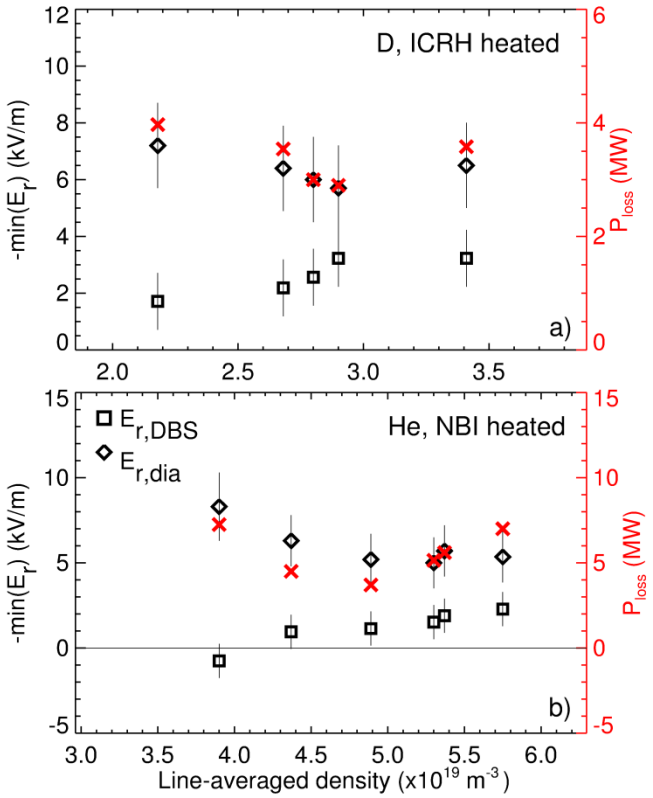

Figure 6: Depth of the diamagnetic term at the L-H transition estimated from the electron kinetic profiles for deuterium ICRH heated (a) and helium NBI heated (b) discharges, together with the L-H power threshold and the E_r minimum measured by DBS. Note the different line-averaged electron density scale in the two plots.

7. Evolution along the heating ramp

The edge $v_\perp$ was studied along the heating ramp used to induce the L–H transition, taking advantage of the unique JET dataset. The temporal evolution of the mean perpendicular velocity radial profiles in deuterium plasmas is presented in figure 7 for selected periods with different ICRH power. Profiles are displayed for two discharges with different line-averaged electron density corresponding to the low and high density branch of the L-H transition. For the lower density discharge, the SOL peak becomes stronger as the input power is ramped up. This is not observed for the discharge with higher density, because the divertor T_e radial gradient is modest throughout the power ramp. As the $v_\perp$ well does not

change significantly along the power ramp in both cases, the differences between the low and high density discharges are mainly related to the behavior of the SOL peak. Interestingly, no significant increase of the shear flow is observed preceding the L–H transition in both cases. In the low density case, the SOL flow is observed to increase when the heating is applied, but then exhibits a modest variation with ICRH power up to the transition (for a time in the order of 1 s). For the high density case, no substantial changes in the edge flow are seen through the entire heating ramp. It is unclear why the $v_\perp$ profile stops evolving when for instance the diamagnetic term estimated from the electron temperature increases by up to a factor of 2 along the power ramp. Note that both the toroidal and poloidal rotation are also expected to evolve along the heating ramp with the balance between the different contributions difficult to anticipate.

CXRS measurements on MAST through the L–H transition at a faster time scale (Δt =200 μs) showed no consistent increase in ∇E_r during the L-mode phase [17]. The E_r evolution along the L-H transition was also previously documented in JET plasmas with carbon wall using CXRS with a time resolution of 50 ms [29]. The E_r profile was reported to remain very flat throughout the L-mode phase and strong edge gradients only started to form after the transition to H-mode. Furthermore, the carbon impurity ion toroidal or poloidal rotation velocities showed no evidence of spin-up prior to the L-H transition. These observations may suggest that the H-mode access is not only established by the mean E_r profile. However, apart from estimating the flow shear, to understand the L-H transition it is also required to characterize the edge turbulence as the characteristics of the edge turbulence may evolve along the heating ramp.

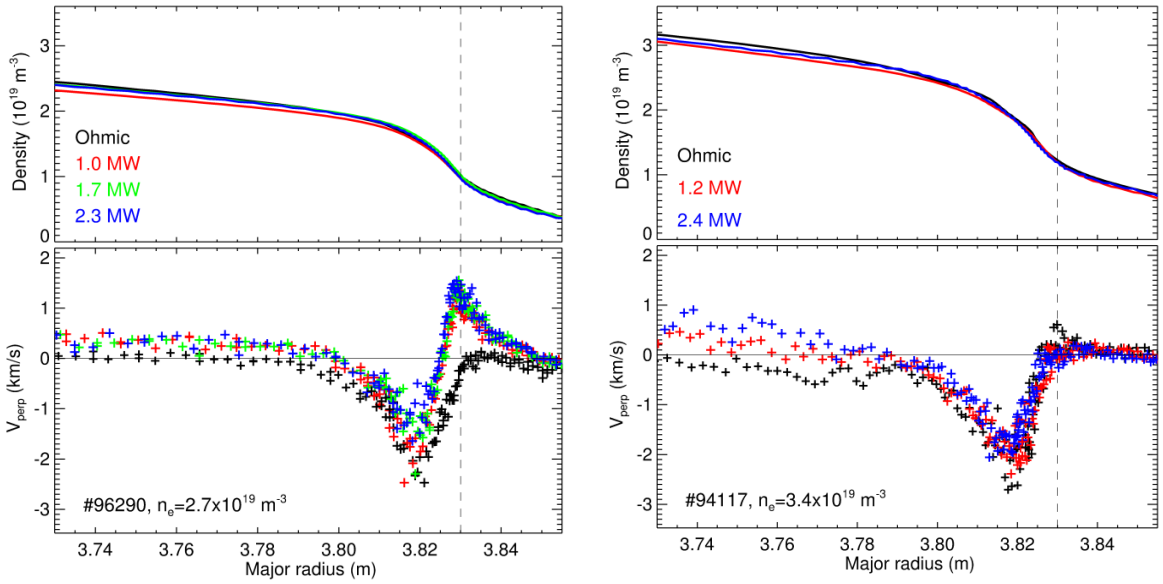

Figure 7: Radial profiles of density and mean perpendicular velocity for deuterium plasmas at different ICRH power levels for discharge #96290 ($\bar{n}$ = 2.7×10^{19} m^{-3}) and #94117 ($\bar{n}$ = 3.4×10^{19} m^{-3}). The separatrix (dashed line) is at 3.83 (±0.01) m. The L–H transition occurs at P_{ICRH} ~2.5 MW for #96290 while for #94117 the transition dithers start at P_{ICRH} ~2.6 MW.

8. Comparison with divertor probe data

The divertor response to the density scan performed in deuterium and helium plasmas is now studied to better understand the behavior of the midplane SOL flow. Spatial profiles of the floating potential, electron temperature and plasma potential at the outer target are compared in figure 8 for three representative helium discharges with different line-averaged electron densities. The plasma potential is derived from the floating potential and the electron temperature assuming a sheath potential drop of $3T_e/e$. Profile positions at the target are mapped to the outboard midplane. Divertor probe data could not be estimated up to the L-H transition for discharge #93903 due to the large electron temperature resulting from the discharge low density and high heating power. Data is shown for $P_{NBI} \approx 3.4$ MW, while the transition occurs at $P_{NBI} \approx 7.4$ MW. As expected, Langmuir probe data at the outer divertor shows a decrease in divertor T_e and T_e radial gradient with increasing line-averaged density. The low probe spatial resolution only allows for a rough estimation of the divertor E_r and therefore a detailed comparison with the midplane profile cannot be performed. It is found that the divertor E_r decreases with density from about 5 kV/m for $\bar{n}$ = 3.9×10^{19} m^{-3} to about 1kV/m for $\bar{n}$ = 5.8×10^{19} m^{-3}, in reasonable agreement with the DBS SOL profiles measured at the midplane. Note that E_r for #93903 should be

underestimated as divertor probe data is obtained far from the transition. For helium plasmas, the outer divertor is attached even for the highest density, as indicated by the electron temperature at the strike-point (around 15 eV).

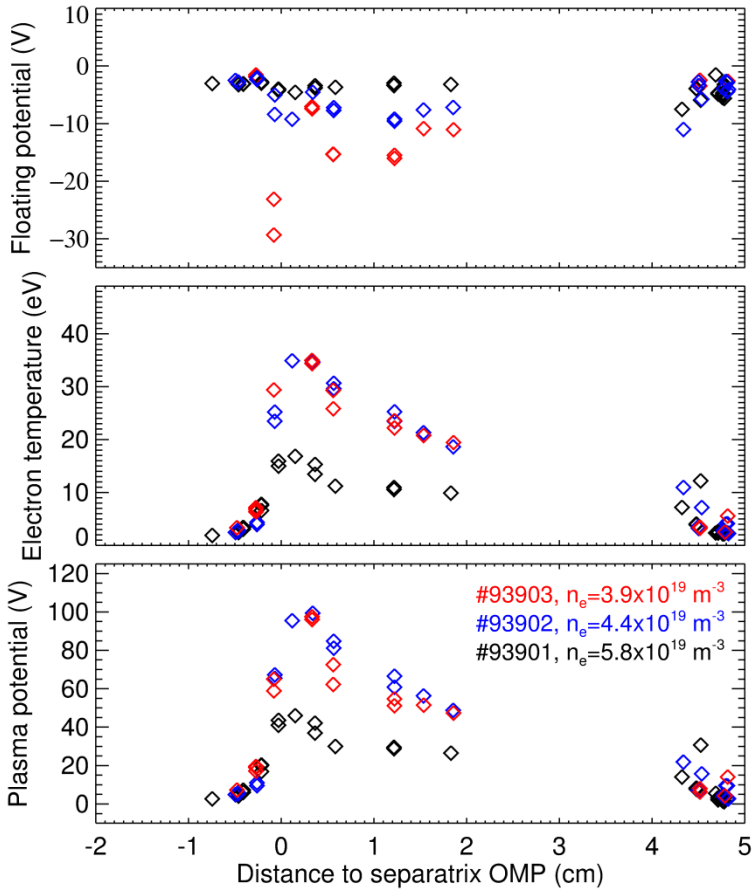

Figure 8: Radial profiles along the outer target of the floating potential, electron temperature and plasma potential at the outer target for three representative helium discharges with different densities. Profile positions at the target are mapped to the outboard midplane.

It is interesting to note that large negative floating potential values with a fine spatial variation are observed for the lowest density discharge, suggesting the presence of strong SOL currents. Currents flowing along the magnetic field are often observed in the divertor region, particularly at low line-averaged density (associated with larger target temperatures) [30, 31]. The existence of SOL currents with a fine spatial structure modifies the plasma potential profile, leading to a large E_r near the outer strike-point that may partially justify the marked SOL peak observed at the midplane for low density helium discharges. This implies that in such cases the E_r profile cannot be simple approximated by $\sim 3\nabla_r T_e/e$. However, the probe spatial resolution does not allow for a detailed characterization of the fine structures induced by the SOL currents. Note that for the

discharges analyzed here, large SOL currents were only observed in low density discharges, possibly due to the combination of a low density with a high P_{LH}.

Finally, the divertor profiles are compared in helium and deuterium plasmas (see figure 9). Discharges with similar density were selected: $\bar{n}$ = 4.4×10^{19} m^{-3} in helium corresponding roughly to the minimum of the P_{LH} curve; and $\bar{n}$ = 4.7×10^{19} m^{-3} in deuterium corresponding the high density branch. Significantly higher divertor temperatures are observed for helium plasmas in spite of the lower input power (He: 93902, $P_{NBI,L-H}$ ~4.4 MW; D: #95312, $P_{NBI,L-H}$ ~5.0 MW), in agreement with the observation that He plasmas exhibit the characteristics of detachment at a higher density. The plasma potential radial gradient is also larger for helium plasmas by a factor around two, partially justifying the larger SOL perpendicular flow observed at the midplane for helium plasmas.

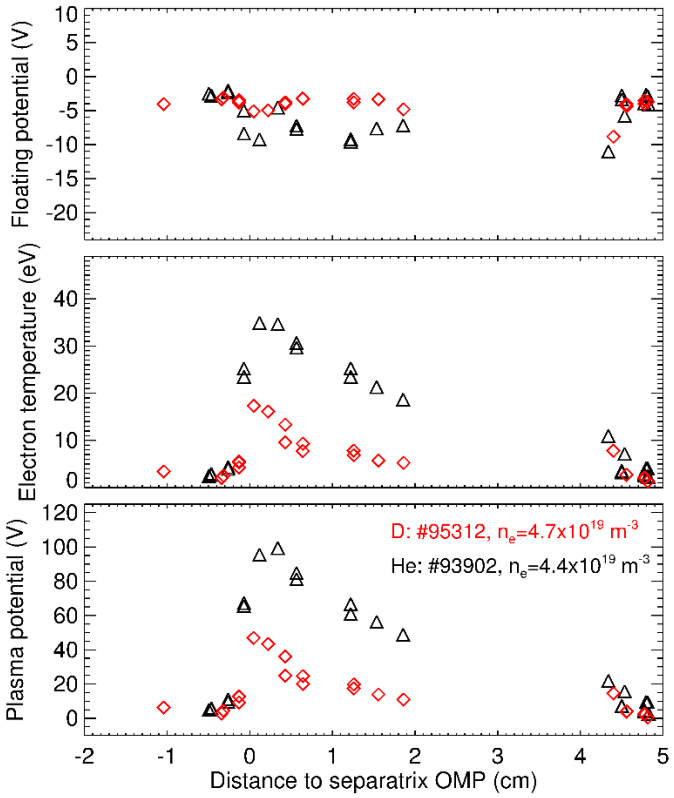

Figure 9: Radial profiles along the outer target of the floating potential, electron temperature and plasma potential at the outer target for deuterium and helium plasma at an intermediate density. Profile positions at the target are mapped to the outboard midplane.

9. Summary

In this work the perpendicular flow is measured at the JET edge plasma by Doppler backscattering for different line-averaged densities in helium and deuterium plasmas aiming at investigating the impact on the L–H transition. The $v_\perp$ profile in the low density branch of the L-H transition has a modest or even no well and a marked outer peak near the separatrix in NBI heated discharges for both D and He plasmas, the SOL peak being sharper for He plasmas. As the line-averaged electron density increases, the SOL $v_\perp$ peak decreases leading to a reduction of the outer $E_r \times B$ shear. The evolution of the SOL peak is in agreement with the modifications in the divertor conditions and in particular with the reduction of the target electron temperature radial gradient with line-averaged electron density. The electron temperature radial gradient at the divertor target is also higher for helium plasmas, justifying the larger SOL perpendicular flow observed at the midplane in helium. A large positive E_r spike near the separatrix was also seen in modelling results, depending on divertor conditions and ion mass [14]. Modelling showed larger positive E_r spikes in the near SOL under conditions where the H-mode power threshold is lower, although no simulations were performed for He plasmas. However, no clear evidence for the importance of the outer shear is found in our experiment and no correlation is found between the power threshold and the outer shear.

Contrary to the SOL peak, the $v_\perp$ well becomes deeper with line-averaged electron density. Nevertheless, even in the high density branch, a shallow $v_\perp$ well is found at the L-H transition, $v_\perp \sim 1.5$ km/s, which is lower by a factor of about two than the contribution from the diamagnetic term estimated from the electron temperature. This indicates that either the edge poloidal and/or toroidal velocities also have a relevant contribution to the perpendicular flow or that the diamagnetic term is overestimated by assuming $T_i = T_e$. The diamagnetic term is likely to be the most relevant in the force balance equation for the L-H transition due to its large amplitude and location (position where the edge shear is found).

Although in general no evidence for the existence of a critical $v_\perp$ is found at JET, the diamagnetic contribution does not vary significantly with density (except for low density helium plasmas), which may indicate that the kinetic profiles are similar at the transition. The variation of the DBS-measured $v_\perp$ minimum with line-averaged density may be explained by the existence of an edge toroidal flow mainly relevant at low density.

The $E \times B$ flow shear was estimated from the $v_\perp$ profile in the inner and outer shear regions. Our results indicate that a critical value of the inner shear might exist for deuterium

plasmas but not for helium plasmas. Furthermore, the outer shear alone does not appear to play a major role in defining the L-H power threshold as it varies with density. For the datasets analyzed here, the average shear in the region just inside the separatrix, including both the inner and outer shear, appears to be a more relevant quantity to access H-mode.

The edge $v_\perp$ profile is similar in deuterium NBI and ICRH heated plasmas except at low density in the region inside separatrix, possibly due to the plasma rotation induced by NBI. As no significant difference in P_{LH} is found between NBI heated and ICRH heated L–H transitions in deuterium plasmas, our results suggest that the shear associated with edge toroidal velocity is small and therefore would correspond to an offset in the flow profile not relevant for the shear required for the transition, at least for deuterium plasmas where the P_{LH} is low. This hypothesis is consistent with previous observation at JET that the flow shear driven by the toroidal rotation profile does not appear to play a role in setting the edge transport barrier [12, 25].

No significant change in the edge perpendicular velocity seems to occur preceding the L-H transition, while the diamagnetic term is evolving along the power ramp. The temporal resolution of the measurements for each probing frequency is only ~300 ms for the diagnostic settings used in this experiment and the fast dynamics near the transition cannot be studied. Therefore, the possibility of a transition triggered by a transient shear below this time scale cannot be excluded. The temporal resolution required to demonstrate the importance of sheared flows for L-H transition studies is demanding, ideally down to turbulence time scales. However, as no evolution in the $v_\perp$ profiles is seen along the power ramp for time scales in the order of 1 s, changes at turbulence time scales are not expected to play a significant role.

Acknowledgements

This work has been carried out within the framework of the EUROfusion Consortium and has received funding from the Euratom research and training programme 2014-2018 and 2019-2020 under grant agreement No 633053. IST activities also received financial support from “Fundação para a Ciência e Tecnologia” through projects UIDB/50010/2020 and UIDP/50010/2020. The views and opinions expressed herein do not necessarily reflect those of the European Commission. Additionally, work was supported in part by the Spanish National Plan for Scientific and Technical Research and Innovation 2017-2 020, grant number FIS2017-85252-R

References

[1] Y.R. Martin et al., J. Phys.: Conf. Ser. 123 (2008) 012033

[2] ITER Research Plan, ITER Organization, 2018 (https://www.iter.org/doc/www/content/com/Lists/ITER%20Technical%20Reports/Attachments/9/ITER-Research-Plan_final_ITR_FINAL-Cover_High-Res.pdf)

[3] D.C. McDonald et al., Plasma Phys. Control. Fusion 46 519 (2004)

[4] E. Righi et al., Nucl. Fusion 39 (1999) 309

[5] F. Ryter et al., Nucl. Fusion 49 (2009) 062003

[6] R. Behn et al., Plasma Phys. Control. Fusion 57 (2015) 025007

[7] P. Gohil et al., Nucl. Fusion 50 (2010) 064011

[8] R.J. Groebner et al., Nucl. Fusion 41(12) (2001) 1789

[9] K.H. Burrell et al., Plasma Phys. Control Fusion 31(10) (1989) 1649

[10] R.J. Taylor et al., Phys. Rev. Lett. 63 (1989) 2365

[11] C. Silva et al., Plasma Phys. Control. Fusion 48 (2006) 727

[12] C.F. Maggi et al., Nucl. Fusion 54 (2014) 023007

[13] E. Delabie et al., "Overview and interpretation of L-H threshold experiments on JET with the ITER-like Wall" [EX/P5-24], paper presented at 25th IAEA Int. Conf. on Fusion Energy St Petersburg 2014

[14] A.V. Chankin et al., Plasma Phys. Control. Fusion 59 (2017) 045012

[15] M. Cavedon et al., Nucl. Fusion 57 (2017) 014002

[16] M. Cavedon et al., Nucl. Fusion 60 (2020) 066026

[17] H. Meyer et al., Nucl. Fusion 51 (2011) 113011

[18] U. Plank et al., Nucl. Fusion 60 (2020) 074001

[19] E.R. Solano et al, "L-H transition studies in Helium plasmas at JET", private communication

[20] G.D. Conway et al., Plasma Phys. Control. Fusion 46 (2014) 951

[21] P. Manz et al., Plasma Phys. Control. Fusion 60 (2018) 085002

[22] E. Poli et al., Computer Physics Communications 136 (2001) 90

[23] J.C. Hillesheim et al., Proc. 12th Inter. Reflectometry Workshop, IRW12, Juelich, Germany (2015)

[24] C. Silva et al., Nucl. Fusion 56 (2016) 106026

[25] J.C. Hillesheim et al., "Implications of JET-ILW L-H Transition Studies for ITER". Preprint: 2018 IAEA Fusion Energy Conference, Gandhinagar [EX/4-1]

[26] H. Meyer et al., Proceedings of 41st European Physics Society Conference on Plasma Physics, P1.013 (2014)

[27] F. Ryter et al., Nucl. Fusion 54(8) (2014) 083003

[28] M. Kocan et al., J. Nucl. Mater. 415 (2011) S1133

[29] Y. Andrew et al., EPL 83 (2008) 15003

[30] C. Silva et al., J. Nucl. Mater. 266-269 (1999) 679

[31] G.M. Staebler and F L Hinton, Nucl. Fusion 29 (1989) 1820